Chemistry and Physics of Lipids 221 (2019) 8–14

Contents lists available at ScienceDirect

Chemistry and Physics of Lipids

journal homepage: www.elsevier.com/locate/chemphyslip

# Effects of lipid composition on the structural properties of human serum amyloid A in reconstituted high-density lipoprotein particles

Hiroka Takase[a,b], Masafumi Tanaka[a,c,*], Yuki Nakamura[a], Shin-ya Morita[d], Toshiyuki Yamada[e], Takahiro Mukai[a]

[a] Laboratory of Biophysical Chemistry, Kobe Pharmaceutical University, Kobe, 658-8558, Japan
[b] Radioisotope Research Laboratory, School of Pharmacy, Kitasato University, Shirokane, Minato-ku, Tokyo, 108-8641, Japan
[c] Laboratory of Functional Molecular Chemistry, Kobe Pharmaceutical University, Kobe, 658-8558, Japan
[d] Department of Pharmacy, Shiga University of Medical Science Hospital, Otsu, 520-2192, Japan
[e] Department of Clinical Laboratory Medicine, Jichi Medical University, Shimotsuke, 329-0498, Japan

ARTICLE INFO

*Keywords:*
Serum amyloid A
Lipid composition
High-density lipoprotein
Apolipoprotein

ABSTRACT

Serum amyloid A (SAA) is a member of exchangeable apolipoproteins that predominantly exists as a component of high-density lipoproteins (HDL). During inflammation, SAA displaces apolipoprotein A–I from HDL and becomes the major protein constituents of HDL. In addition, HDL lipid composition is altered in response to inflammation, which may induce the structural reorganization of SAA and affect its function. Therefore, the physiological roles of HDL can be influenced by changes in their protein and lipid compositions that are triggered by inflammatory diseases. Here, the effect of HDL lipid composition on the structural properties of SAA was examined. Uniformly sized reconstituted HDL (rHDL) was prepared and mainly composed of phosphatidylcholine with a single additional lipid species. Results showed that changes in lipid composition had no significant impact on the helical content of SAA and its thermodynamic stability. However, rHDL lipid composition affected other structural properties of SAA, such as its tryptophan microenvironment and kinetic stability, and thus influenced the susceptibility of SAA to enzymatic digestion. Therefore, changes in HDL lipid composition may affect the physiological function of SAA and the pathogenesis of SAA-related diseases.

## 1. Introduction

High-density lipoproteins (HDL) are heterogeneous particles that are composed of various proteins and lipids. HDL has been reported to exert protective effects against cardiovascular diseases because of their anti-inflammatory, antioxidative, and reverse cholesterol transport activities (Lund-Katz and Phillips, 2010). Therefore, several preclinical and clinical trials have been conducted to assess the effects of increased HDL levels. However, further studies explained that the protective effects of HDL depend on its quantity and quality because the atheroprotective activities of HDL are regulated by differences in HDL composition. Apolipoprotein (apo) A-I is a major protein component of HDL that is considered to be crucial for these functions. Serum amyloid A (SAA) levels are markedly increased during inflammation and can form SAA-enriched HDL through apo A-I displacement (Hoffman and Benditt, 1982; Khovidhunkit et al., 2004; Tolle et al., 2012). Therefore, SAA localization on HDL may influence cardiovascular disease risks. Acute-phase HDL that contains increased SAA levels exhibits pro-inflammatory properties (Tolle et al., 2012; van der Westhuyzen et al., 2007). On the other hand, it has been reported that the lipid composition of HDL is altered in several disease conditions (Gomez Rosso et al., 2014; Marsche et al., 2014; Morgantini et al., 2014), which may affect HDL function directly or indirectly by altering protein conformations. Therefore, the quality of HDL could be regulated by both their lipid and protein compositions that are altered by various physiological or pathological conditions.

The detailed structure of SAA within HDL is yet to be determined; however, SAA has been shown to share several structural characteristics with other apolipoproteins. For example, SAA can form a membrane-binding amphipathic helix, which is an important structural motif

*Abbreviations:* apo, apolipoprotein; CD, circular dichroism; Chol, cholesterol; HDL, high-density lipoprotein; MMP-1, matrix metalloproteinase-1; PA, phosphatidic acid; PC, phosphatidylcholine; PE, phosphatidylethanolamine; PS, phosphatidylserine; SAA, serum amyloid A; SM, sphingomyelin; Trp, tryptophan

* Corresponding author at: Laboratory of Functional Molecular Chemistry, Kobe Pharmaceutical University, 4-19-1 Motoyamakita-machi, Higashinada-ku, Kobe, 658-8558, Japan.
*E-mail address:* masatnk@kobepharma-u.ac.jp (M. Tanaka).

https://doi.org/10.1016/j.chemphyslip.2019.03.001
Received 8 February 2019; Received in revised form 27 February 2019; Accepted 1 March 2019
Available online 02 March 2019
0009-3084/ © 2019 Elsevier B.V. All rights reserved.

found in lipid-associating proteins (Segrest et al., 1976). Furthermore, the crystal structure of SAA has a four-helix bundle fold (Lu et al., 2014) similar to that observed in other apolipoproteins (Pollard et al., 2013; Wilson et al., 1991). However, it has been reported that lipid-free human SAA is mostly unstructured in aqueous solution at physiological temperatures and induces α-helical structures upon lipid binding (Takase et al., 2014), which has additionally been verified in murine SAA (Jayaraman et al., 2015). Similar to other apolipoproteins, the function of SAA may be modulated by the lipid composition upon lipid binding (Bergeron et al., 1995; Narayanaswami and Ryan, 2000). However, it remains unclear how changes in HDL lipid composition caused by chronic inflammatory conditions can influence the structural properties and biological functions of SAA.

SAA is a precursor of amyloid fibrils that are formed in patients with amyloid A (AA) amyloidosis, a complication of chronic inflammatory diseases (Lachmann et al., 2007; Uhlar and Whitehead, 1999; Westermark and Westermark, 2009). Lipid binding has been observed to greatly influence fibril formation of amyloidogenic proteins. However, the combination of protein and lipid species encountered upon lipid binding could determine whether facilitative or inhibitory effects ensue (Butterfield and Lashuel, 2010; Ryan et al., 2011). For example, the interaction of SAA with neutral phospholipids has been observed to prevent fibril formation by stabilizing an α-helical structure; however, SAA interaction with acidic phospholipids appeared to promote fibril formation (Tanaka et al., 2017). Therefore, the structural properties of SAA that are modulated by HDL lipid composition may elucidate the pathogenesis of AA amyloidosis.

The present study aimed to evaluate the structural characteristics, particularly the secondary structure, microenvironment, and conformational stability, of SAA bound to HDL with controlled lipid compositions. Furthermore, the susceptibility of SAA to enzymatic digestion was assessed upon HDL binding, which is influenced by its structure. The findings may contribute toward the elucidation of the potential functional implications of SAA in lipid metabolism and aid the understanding of SAA-related disease pathogenesis.

## 2. Materials and methods

### 2.1. Materials

1-Palmitoyl-2-oleoyl-phosphatidylcholine (PC) and cholesterol (Chol) were purchased from NOF Corporation (Tokyo, Japan) and Sigma–Aldrich (St. Louis, USA), respectively. Phosphatidic acid (PA, egg extract), phosphatidylethanolamine (PE, egg extract), phosphatidylserine (PS, brain extract), and sphingomyelin (SM, brain extract) were purchased from Avanti Polar Lipids (Alabaster, USA).

### 2.2. SAA protein preparation

The recombinant SAA protein (corresponding to human SAA1.1 with an extra N-terminal methionine) was expressed in *Escherichia coli* and purified as previously described (Yamada and Wada, 2003). Purified protein solutions were dialyzed from 4 M urea into 20 mM Tris-HCl buffer (pH 7.4) and centrifuged to remove insoluble or aggregated matter prior to use. Samples were stored at 4 °C throughout the preparation procedure. Protein concentrations were determined by the Lowry method using bovine serum albumin (Bio-Rad, Hercules, USA) as a standard.

### 2.3. Preparation and characterization of reconstituted HDL (rHDL)

rHDL composed of SAA and various lipids were prepared by the cholate dialysis method. In brief, vacuum dried lipids (PC alone or mixed with one additional lipid [Chol, SM, PE, PS, or PA] at an initial molar ratio of 80:20) were solubilized by adding sodium cholate to a final concentration of 20 mM. The solubilized lipids were then incubated with SAA at a lipid to protein weight ratio of 1:1 for 2 h at room temperature. Ternary mixtures were extensively dialyzed against 20 mM Tris-HCl buffer (pH 7.4) to remove the cholate. Lipid-SAA complexes were then loaded onto a Superdex 200 gel filtration column (60 × 1.6 cm) and were eluted with 20 mM Tris-HCl buffer (pH 7.4) at a flow rate of 1 mL/min using a Biologic FPLC (Bio-Rad, Hercules, USA). The lipid compositions of the eluted rHDL were determined using an enzyme-based Amplex Red fluorometric assay, as previously described (Morita et al., 2012a, b; Morita et al., 2010, 2009). Chol concentrations of rHDL were determined using a cholesterol fluorometric assay kit (Cayman Chemical, Ann Arbor, USA). A dynamic light scattering (DLS) technique was used to estimate rHDL sizes with a Zetasizer Nano ZS (Malvern, Worcestershire, UK) at 25 °C. Particle diameters were represented by the number mean.

### 2.4. Fluorescence quenching

Fluorescence measurements were performed at 37 °C using a Hitachi F-7000 fluorescence spectrophotometer (Hitachi, Tokyo, Japan). Tryptophan (Trp) emission fluorescence spectra of the protein samples (25 μg/mL) were recorded from 300 to 420 nm at an excitation wavelength of 295 nm using 4 × 4 mm quartz cuvettes. Fluorescence measurements were conducted with increasing concentrations of potassium iodide (0–0.56 M) by adding a 5 M stock solution containing 200 μM sodium thiosulfate to suppress triiodide ($I_3^-$) formation (Lehrer, 1971; Rohamare and Gaikwad, 2014).

### 2.5. Circular dichroism (CD) spectroscopy

CD measurements were performed at a 25 μg/mL protein concentration using a Jasco J-820 spectropolarimeter (Hachioji, Japan). CD spectra obtained at 37 °C were corrected by subtracting the baseline of a blank sample. The mean residual ellipticity ($[\theta]$) was calculated as previously described (Tanaka et al., 2017). For the gradual heating experiments, changes in $[\theta]$ at 222 nm ($[\theta]_{222}$) were monitored at a protein concentration of 25 μg/mL, as the sample was heated at 1 °C/min over a temperature range of 4 °C – 100 °C. For temperature-jump (T-jump) experiments, $[\theta]_{222}$ were recorded beginning from 25 °C, followed by a rapid temperature increase up to 45 °C – 80 °C. The T-jump data were fitted using exponential curves and the obtained kinetic constants were analyzed using an Arrhenius model.

### 2.6. Transmission electron microscopy (TEM)

Freshly prepared rHDL samples were adsorbed onto 400-mesh formvar film coated copper grids before staining with 2% (w/v) ammonium molybdate. The grids were imaged using a JEM-1400Plus transmission electron microscope equipped with a CCD camera (JEOL, Akishima, Japan).

### 2.7. Matrix metalloproteinase-1 (MMP-1) digestion

MMP-1 was purchased from Sigma–Aldrich (St. Louis, USA). SAA solution (25 μg/mL) was mixed with the reaction buffer (20 mM Tris, 150 mM NaCl, 5 mM $CaCl_2$, and 1 mM $ZnCl_2$, pH 7.6) containing 350 nM MMP-1 and incubated at 37 °C for specific time periods (0.5, 1, 2, 4, and 24 h). Reactions were terminated by boiling for 5 min, and the samples were analyzed by SDS-PAGE using a Tris-tricine buffer system.

## 3. Results and discussion

### 3.1. Preparation of SAA-HDL particles with different lipid compositions

To examine the effect of lipid compositions on rHDL particle characteristics, six different types of rHDL particles composed of PC alone or mixed with one additional lipid species were prepared. Previously, the

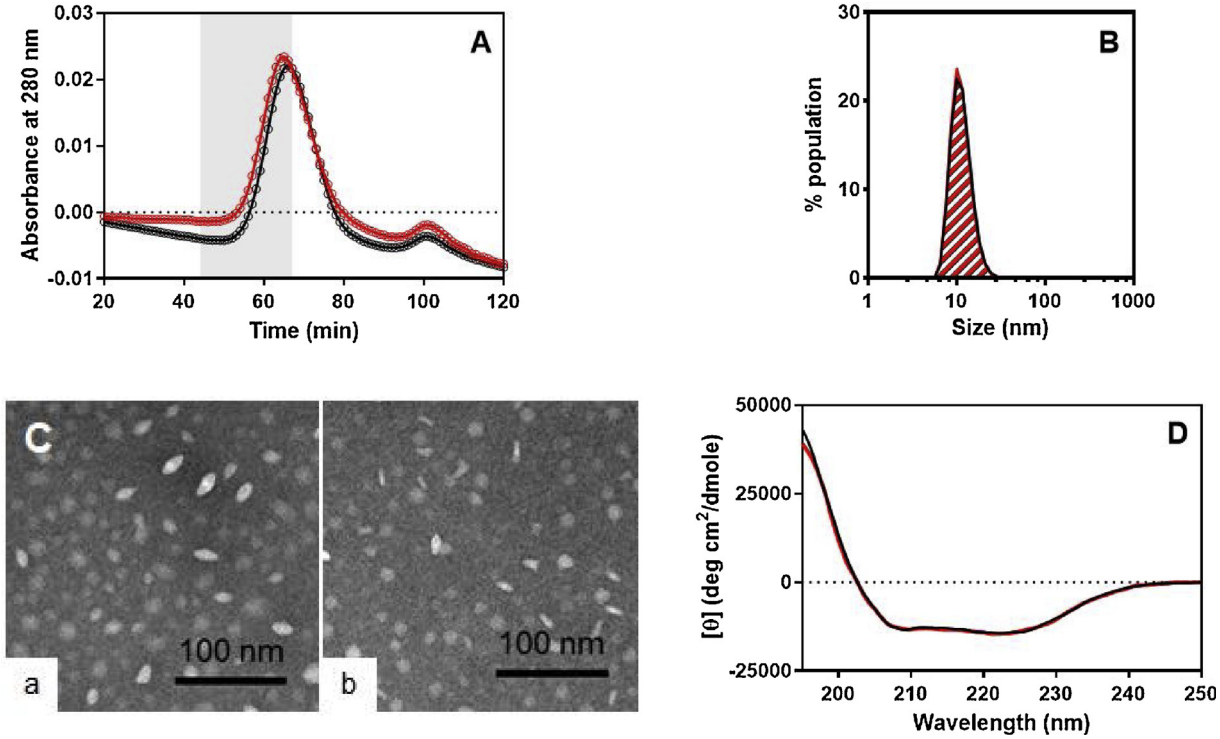


**Fig. 1.** (A) Representative gel filtration elution profiles of PC-SAA (black) and PC/Chol-SAA (red) complexes monitored by UV absorbance at 280 nm. Elution position of human plasma HDL is indicated by gray background. (B) Size distributions of PC-SAA (black) and PC/Chol-SAA (red) complexes at 25 °C. (C) Transmission electron micrographs of PC-SAA (a) and PC/Chol-SAA (b) complexes. (D) CD spectra of PC-SAA (black) and PC/Chol-SAA (red) complexes at 37 °C.

physicochemical properties of rHDL composed of SAA and dimyristoylphosphatidylcholine (DMPC) have been examined (Takase et al., 2014). DMPC is frequently used as an rHDL lipid component because its gel-to-liquid crystalline phase transition temperature (approximately 25 °C) enables spontaneous vesicle solubilization that results in rHDL formation. However, the lipid species that can be used for rHDL formation by this method are highly limited because the phase transition temperatures of physiologically relevant phospholipids are usually below 0 °C. Therefore, the cholate dialysis method was used to prepare rHDL particles containing various lipid species.

Fig. 1A shows representative gel filtration elution profiles of PC-SAA and PC/Chol-SAA complexes. PC-SAA complexes prepared by the cholate dialysis method showed a broader peak than DMPC-SAA complexes prepared by spontaneous vesicle solubilization (Takase et al., 2014). In addition, the presence of Chol had little effect on the overall peak shape corresponding to each rHDL particle. As shown in Figure S1 A, with the exception of the major peak of PC/PA-SAA complexes that eluted slightly later than the other complexes, all lipid-SAA complexes exhibited similar elution profiles with a comparable half-width. The fractions comprising and surrounding the major elution peak were used for the subsequent experiments.

Further, enzymatic methods were used to analyze the lipid compositions of the rHDL particle eluates following gel filtration (Table 1). The incorporation rates of additional lipids mixed with PC into rHDL were dependent on the species. For example, glycerophospholipids (PE, PS, and PA) were incorporated into lipid-SAA complexes at a ratio that was approximately equivalent to the initial ratio. In contrast, the PC/Chol-SAA and PC/SM-SAA complexes contained higher contents of Chol (35%) and SM (27%) than those in the initial ratio. Chol was expected to be incorporated into rHDL at a lower rate because it could be removed during dialysis process due to its slight water solubility. The higher Chol and SM contents may be associated with membrane fluidity because they have a more compact molecular structure than PC, which can cause the rigidification of fluid membranes. Furthermore, as amyloid fibrils derived from SAA contain lipids rich in Chol and SM (Gellermann et al., 2005), SAA may preferentially associate with raft lipids.

### 3.2. Characterization of SAA-HDL particles with different lipid compositions

Next, DLS was used to measure rHDL particle sizes (Table 1). Number-averaged size distributions of PC-SAA and PC/Chol-SAA complexes largely overlapped and were homogeneous (Fig. 1B). Particle diameters of PC-SAA complexes were approximately 10–13 nm, which were slightly larger than those of DMPC-SAA complexes that were previously prepared by spontaneous vesicle solubilization (Takase et al., 2014). The particle sizes of all lipid-SAA complexes were within the range of 10–14 nm (Fig. S1B), which corresponds to the size of native HDL. Any heterogeneous populations of lipid-SAA complexes that may have formed immediately after the cholate dialysis could have been eliminated by gel filtration.

The morphology of rHDL particles were then examined using TEM. TEM images of PC-SAA and PC/Chol-SAA complexes showed typical patterns of circular and rectangular mixtures, which correspond to the top and side views of rHDL particles, respectively (Fig. 1C). This suggests that, similar to nascent HDL, their overall shapes were discoidal. These results are inconsistent with those of a previous report, which showed that murine SAA formed HDL-sized lipid complexes with a distorted bilayer conformation that differed from the characteristic structures formed in the discoidal assembly (Frame et al., 2017), despite its high sequence homology (approximately 75%) to human SAA. Furthermore, rHDL particles prepared with other additional lipids were discoidal in shape, with only minor differences in overall particle diameters compared with the diameters of PC-SAA and PC/Chol-SAA complexes (Fig. S1C).

The CD spectra of PC-SAA and PC/Chol-SAA complexes are shown in Fig. 1D. These exhibit two minimal values at 208 and 222 nm, which is characteristic of an α-helical structure. The helical content of SAA in these complexes was calculated to be approximately 45% (Table 1),

**Table 1**
Characteristics of rHDL composed of SAA and various lipids.

| Lipid composition in SAA-HDL | Final molar content of added lipid (%) | Molar ratio of PC/added lipid to SAA | Diameters (nm) | Helical content[a] (%) |
|---|---|---|---|---|
| Lipid-free[b] | | | | 16.0 ± 0.7 |
| PC | | 12.1 ± 4.8 | 11.6 ± 1.7 | 44.3 ± 6.6 |
| PC/Chol | 34.9 ± 0.9 | 6.4 ± 0.8 / 3.4 ± 0.4 | 11.4 ± 1.2 | 44.9 ± 1.6 |
| PC/SM | 27.1 ± 7.8 | 9.1 ± 4.2 / 3.3 ± 1.7 | 11.8 ± 1.9 | 46.0 ± 2.8 |
| PC/PE | 16.5 ± 3.2 | 8.3 ± 1.6 / 1.6 ± 0.2 | 13.1 ± 1.2 | 38.7 ± 2.9 |
| PC/PS | 17.3 ± 3.7 | 8.1 ± 3.1 / 1.8 ± 1.0 | 11.2 ± 1.2 | 39.9 ± 2.2 |
| PC/PA | 18.4 ± 2.1 | 11.6 ± 4.7 / 2.5 ± 0.8 | 11.1 ± 1.3 | 45.5 ± 6.2 |

[a] The α-Helical contents were calculated as follows: % α-helix = $[(-[\theta]_{222} + 3000)/(36{,}000 + 3000)] \times 100$.
[b] Data are from (Takase et al., 2014) obtained in 10 mM sodium phosphate (pH 7.4).

which appeared to be inconsistent with a previous study using SAA fragment peptides, which reported that only the N-terminal region of SAA can bind to lipids (Ohta et al., 2009). However, X-ray crystallographic data have indicated that the central region of SAA forms an α-helical structure (Lu et al., 2014). Therefore, initial binding of the SAA N-terminal region to lipids can induce a conformational change, similar to that proposed in other apolipoproteins (Fisher and Ryan, 1999; Saito et al., 2003). SAA in the other lipid-SAA complexes showed almost similar spectra (Fig. S1D). Approximately 4–7% decrease in the SAA helical content of PC/PE-SAA and PC/PS-SAA complexes corresponds to the loss of 4–7 helical residues. A previous study that suggested that the secondary structure of the central region of SAA is sensitive to changes in lipid composition (Tanaka et al., 2017). Therefore, α-helix formation in this region may be partially disrupted in these complexes.

In summary, there are no substantial differences between the prepared rHDL particles, regardless of their compositions, in terms of particle sizes and morphologies. Furthermore, the lipid compositions of these rHDL particles have no significant influences on the secondary structures of SAA.

### 3.3. Effect of SAA-HDL lipid compositions on the SAA microenvironment

The SAA molecule has three Trp residues at positions 18, 53, and 85. Trp fluorescence quenching experiments were performed at 37 °C to examine the effects of lipid composition on the SAA local microenvironment. Fig. 2A shows representative spectra that reveal decreases in the SAA Trp fluorescence intensity upon the introduction of KI as a quencher. The wavelength of maximum fluorescence (WMF) in the absence of KI is summarized in Table 2. Subsequently, the quenching data was analyzed using the Stern–Volmer equation: $F_0/F = 1 + K_{SV}[Q]$, where $F_0$ and $F$ are the fluorescence intensities in the absence and presence of the quencher, respectively; and $[Q]$ is the concentration of the quencher in solution (Fig. 2B). The Stern–Volmer quenching constant ($K_{SV}$), which is obtained by the slope of the linear regression line, reflects the accessibility of Trp residues to the quencher (Table 2). The $K_{SV}$ value for SAA molecules in the lipid-free state was 2.9 $M^{-1}$, which is approximately fourfold smaller than that of the standard compound, *N*-Ac-Trp-$NH_2$ (approximately 12 $M^{-1}$) (Kolev and Dolashka-Angelova, 2001; Lehrer, 1971). These results show that the Trp residues in lipid-free SAA have limited accessibility to KI, indicating that the Trp residues are partially buried due to possible interactions with adjacent amino acids and/or conformational fluctuations because of the unstructured nature of SAA molecules at 37 °C. Upon lipid binding, the lower shifts of WMF were observed in all rHDL particles. Compared with the lipid-free state, the $K_{SV}$ values for SAA molecules in all rHDL particles were further decreased to approximately 1.0–1.3 $M^{-1}$, except for rHDL (PC/PA) that showed a markedly smaller $K_{SV}$ value (0.6 $M^{-1}$). Because iodide ions act as a negatively charged hydrophilic quencher, the $K_{SV}$ value was predicted to be smaller when a Trp residue is surrounded by a negatively charged or less hydrophilic environment. However, the $K_{SV}$ value for rHDL (PC/PS) was equivalent to those for rHDL (PC) and (PC/PE). Therefore, the smaller $K_{SV}$ value for rHDL (PC/PA) is not merely because of the negatively charged head group in the PA molecule. Intriguingly, PA has been revealed to specifically induce local conformational changes in other proteins (Jiang et al., 2015; Ouyang et al., 2003; Raja et al., 2007). Therefore, the decreased $K_{SV}$ value in rHDL (PC/PA) may suggest that the local conformation around the Trp residues is distinct from that in rHDL composed of other lipids. The linearity of the Stern-Volmer plots suggests that the three Trp residues remotely located across the 104-residue SAA molecule (at residues 18, 53, and 85) have similar solvent-accessibility. Further studies using SAA mutants with only a single Trp may clearly

**Table 2**
WMF and KI quenching parameters.

| Lipid composition in SAA-HDL | WMF (nm) | $K_{SV}$ ($M^{-1}$) |
|---|---|---|
| Lipid-free | 343.7 ± 1.8 | 2.9 ± 0.7 |
| PC | 333.9 ± 0.6 | 1.0 ± 0.2 |
| PC/Chol | 332.5 ± 0.7 | 1.3 ± 0.1 |
| PC/SM | 332.4 ± 1.0 | 1.2 ± 0.1 |
| PC/PE | 334.4 ± 1.4 | 1.0 ± 0.1 |
| PC/PS | 334.3 ± 2.3 | 1.0 ± 0.2 |
| PC/PA | 334.4 ± 1.5 | 0.6 ± 0.1 |

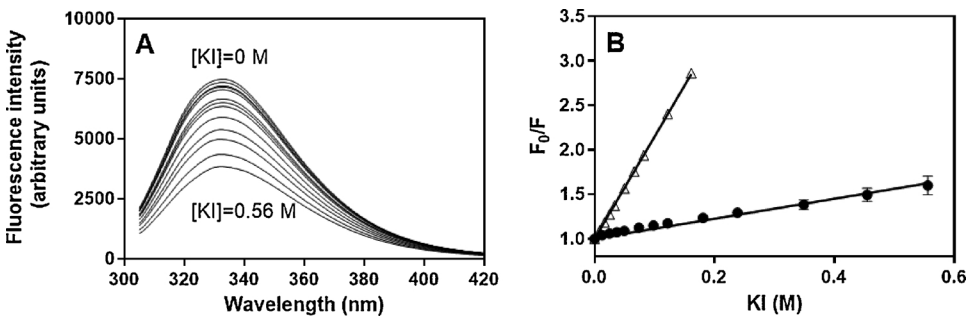


**Fig. 2.** (A) Representative Trp fluorescence spectra of SAA in rHDL (PC) showing the quenching effect of increasing concentrations of KI (0–0.56 M) at 37 °C. (B) Stern–Volmer plot for quenching of SAA Trp fluorescence with KI in rHDL (PC). Data for *N*-Ac-Trp-$NH_2$ quenching are also depicted for comparison (triangles).

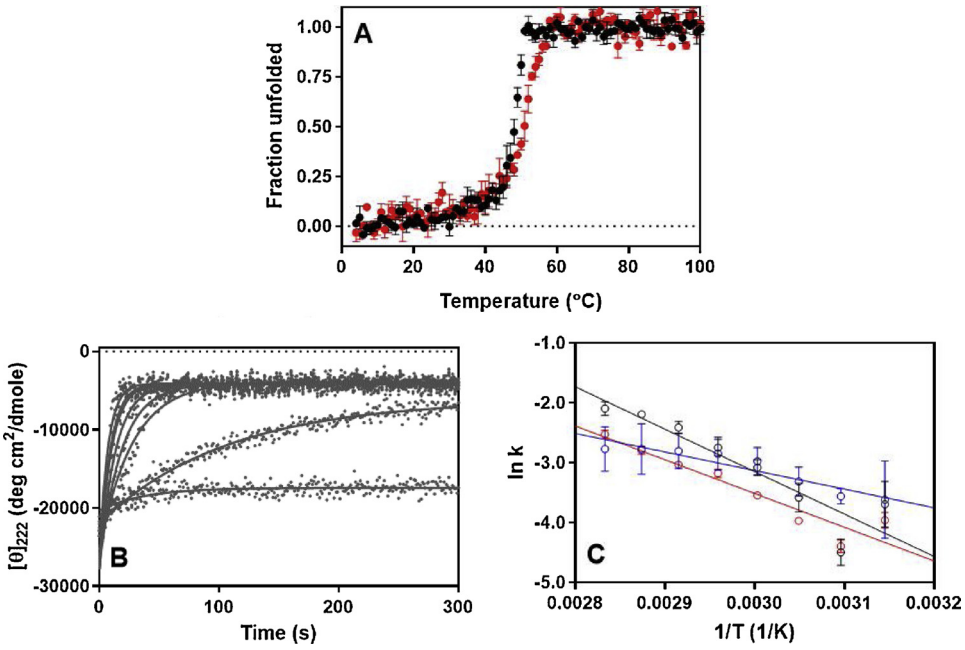


**Fig. 3.** (A) Thermal denaturation curves of rHDL (PC) (black) and rHDL (PC/Chol) (red) monitoring changes at 222 nm ($[\theta]_{222}$). (B) Representative kinetic CD data of SAA in rHDL (PC) particles recorded in T-jumps from 25 °C to 45–80 °C. The data were plotted in order of increasing temperature ( + 5 °C) from the bottom. (C) Arrhenius plots (ln $k$ versus $1/T$) for SAA denaturation in rHDL (PC) (black), rHDL (PC/Chol) (red), and rHDL (PC/PS) (blue).

reveal the specific residue(s) that are less susceptible to the quencher in various forms of rHDL.

### 3.4. Effect of SAA-HDL lipid compositions on the conformational stability of SAA

The temperature-dependent denaturation of SAA molecules in rHDL was examined by monitoring the $[\theta]_{222}$ values obtained from CD measurements as an indicator of the α-helical structure. Fig. 3A shows the thermal denaturation sigmoidal curves of the SAA protein in rHDL (PC) and (PC/Chol), which depict a steep slope that rises at approximately 40 °C. These denaturation behaviors closely resemble that of rHDL (DMPC) (Takase et al., 2014). The observation that the incorporation of Chol into rHDL has little impact on the conformational stability of human SAA is consistent with the results of a previous study using murine SAA (Frame et al., 2017). rHDL particles composed of other additional lipids showed similar thermal denaturation patterns (Fig. S1E). The $T_{1/2}$ values, which are the temperatures at which half of the total change in the SAA protein CD signal is observed, were approximately 50 °C for all rHDL particles, regardless of lipid composition (Table 3). These values are considerably smaller than $T_{1/2}$ values recorded for other apolipoproteins in rHDL (e.g. approximately 80 °C for apo A-I) (Fang et al., 2003; Jayaraman et al., 2005). Even apoC-I, which has a lower molecular weight than SAA, exhibited a higher $T_{1/2}$ value (Gursky and Ranjana, 2002), suggesting that the low conformational stability of SAA is not because of its small molecular size but because of its low lipid affinity. SAA showed a lower helical content than other apolipoproteins, even in the presence of lipids (Table 1). It is likely that less helical regions are in contact with lipids. Therefore, the lower $T_{1/2}$ values for SAA may be because of the lack of cooperativity that is attributable to multivalent binding.

**Table 3**
SAA thermal denaturation parameters.

| Lipid composition in SAA-HDL | $T_{1/2}$ (°C) | $E_a$ (kJ/mol) |
|---|---|---|
| PC | 47.9 ± 0.5 | 55.5 ± 6.1 |
| PC/Chol | 50.6 ± 0.2 | 46.9 ± 2.5 |
| PC/SM | 50.6 ± 0.7 | 48.0 ± 8.3 |
| PC/PE | 50.2 ± 1.0 | 51.0 ± 8.7 |
| PC/PS | 51.4 ± 2.2 | 25.7 ± 1.9* |
| PC/PA | 49.3 ± 1.4 | 31.4 ± 7.5** |

One sample t-test.
* $p < 0.01$.
** $p < 0.05$ ($n \geq 3$).

Next, an alternative approach was adopted to kinetically analyze rHDL stabilities. The activation energy ($E_a$), which was determined from a correlation between the unfolding rate constant and absolute temperature, was calculated for each rHDL particle to examine its conformational stability (Gursky and Ranjana, 2002). For reference, the $E_a$ value for apo A-I in rHDL has been shown to be approximately 200 kJ/mol (Jayaraman et al., 2005). The time course of SAA thermal denaturation was monitored in each rHDL with a rapid temperature increase. Fig. 3B shows representative T-jump curves of the SAA protein in rHDL (PC). The T-jump data measured at various temperatures were approximated by an exponential model to obtain a rate constant, and then Arrhenius plots were constructed (Fig. 3C). The $E_a$ values calculated from the slopes of the Arrhenius plots are summarized in Table 3. The $E_a$ value of rHDL (PC) was approximately 55 kJ/mol and those of rHDLs (PC/Chol), (PC/SM), or (PC/PE) were approximately 45–50 kJ/mol. In contrast, the $E_a$ values of rHDL particles containing acidic phospholipids (PS or PA) were significantly lower (approximately 25–30 kJ/mol). Protein conformational stability is generally discussed in two different terms: thermodynamic and kinetic stabilities (Quezada et al., 2017). Thermodynamic stability, which was evaluated by gradual heating experiments, reflects static flexibility that indicates a certain protein's ability to change its structure. Kinetic stability, which was evaluated using the T-jump experiments, reflects dynamic flexibility of a protein, suggested by the rate at which a conformational change occurs. Thermodynamic and kinetic stabilities are not necessarily correlated because they refer to different processes. The lower $E_a$ values for rHDL (PC/PS) and (PC/PA) indicate that they are kinetically unstable. This suggests that the incorporation of acidic phospholipids into rHDL particles increases the dynamic flexibility of the SAA molecules.

### 3.5. Effect of SAA-HDL lipid compositions on enzymatic digestion of SAA molecules

To examine the susceptibility of SAA in rHDL to protease digestion, which can be influenced by protein structure, SAA protein molecules in rHDL with different lipid compositions were digested using MMP-1 as a model protease. MMP-1 is an endopeptidase that has been detected

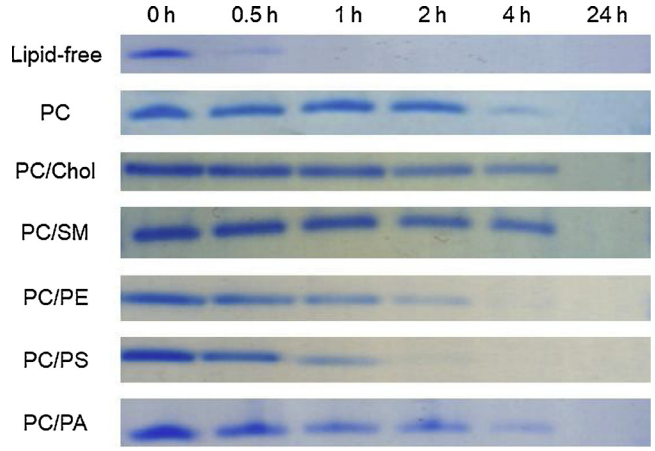


**Fig. 4.** Protease digestion experiments. SAA (25 μg/mL) in lipid-free and rHDL-bound states was incubated with MMP-1 (350 nM) at 37 °C for specific time periods (0.5, 1, 2, 4, and 24 h).

together with SAA fibrils from the lesions in patients with AA amyloidosis (Muller et al., 2000). Fig. 4 shows the time-dependent decreases in the full-length SAA protein (intact polypeptide) bands on SDS-PAGE gels following incubation with MMP-1. Intact SAA in rHDL persisted for a longer time period than lipid-free SAA, suggesting that the lipidation of SAA impedes protease access, which is consistent with the observations of the fluorescence quenching experiments. However, the rate of decrease in the intact band intensity varied depending on the rHDL lipid composition. In particular, bands of the intact SAA protein in rHDL (PC/Chol) and (PC/SM) persisted during a longer incubation period, whereas bands of the intact SAA protein rapidly disappeared in rHDL (PC/PE), (PC/PS), and to a lesser extent (PC/PA). Previous studies have reported that SAA in lipid-rich complexes containing either PE or acidic phosphatidylglycerol were susceptible to tryptic digestion (Jayaraman et al., 2018). These results may reflect the differences in the membrane packing of different rHDL particles. Although it is possible that hydrophobic and/or electrostatic interactions between rHDL and MMP-1 were merely enhanced, it is plausible that a part of the SAA molecule with MMP-1 cleavage sites is exposed when SAA is bound to rHDL containing these phospholipids. It has been reported that the region between residues 51 and 57 in SAA are cleaved by MMP-1 (Stix et al., 2001), which is consistent with the fragmentation pattern of SAA shown in Figure S2. With the structural data, these phospholipids possibly induce subtle but significant structural modifications in the central region of the SAA molecule.

In the present study, it was revealed that changes in rHDL lipid composition modulate the structural properties of the SAA molecule. For example, although the overall helical content of SAA molecules and its thermodynamic stability were unaltered in rHDL, the tryptophan microenvironment and kinetic stability were affected by rHDL lipid compositions. Accordingly, the susceptibility of the SAA molecule to MMP-1 cleavage was altered. Although such dramatic changes in lipid composition may never happen in the human body, it is also true that HDL is enriched in PA under chronic inflammatory conditions, such as rheumatoid arthritis (Gomez Rosso et al., 2014). In addition, mixtures of a wide variety of lipids with different size, charge, or fluidity in HDL under the physiological conditions would yield more complicated and concerted effects. SAA has a well-established function in lipid transport and is implicated in various diseases. Therefore, the present data could aid the understanding of the effects of individual lipid species on the lipid metabolism and the pathogenesis of SAA-related diseases. At present, the protein compositions of lipoproteins are often assessed to monitor some pathological conditions (Diffenderfer and Schaefer, 2014; Shah et al., 2013; Watanabe et al., 2012). Lipid compositional analyses of lipoproteins could be increasingly useful for monitoring the patients' conditions in due course.

## Conflict of interest

(1) All third-party financial support for the work in the submitted manuscript. This work was supported by Grant-in-Aid for JSPS Fellows (15J12051).
(2) All financial relationships with any entities that could be viewed as relevant to the general area of the submitted manuscript. Nothing.
(3) All sources of revenue with relevance to the submitted work who made payments to you, or to your institution on your behalf, in the 36 months prior to submission. Nothing.
(4) Any other interactions with the sponsor of outside of the submitted work should also be reported Nothing.
(5) Any relevant patents or copyrights (planned, pending, or issued) Nothing.
(6) Any other relationships or affiliations that may be perceived by readers to have influenced, or give the appearance of potentially influencing, what you wrote in the submitted work Nothing.

## Acknowledgements

We thank Ms. Akika Murakami and Ms. Saki Ueda for their technical assistance. This work was supported by Grant-in-Aid for JSPS Fellows (15J12051). The authors would like to thank Enago for the English language review.

## Appendix A. Supplementary data

Supplementary material related to this article can be found, in the online version, at doi:https://doi.org/10.1016/j.chemphyslip.2019.03.001.

## References

Bergeron, J., Frank, P.G., Scales, D., Meng, Q.H., Castro, G., Marcel, Y.L., 1995. Apolipoprotein A-I conformation in reconstituted discoidal lipoproteins varying in phospholipid and cholesterol content. J. Biol. Chem. 270, 27429–27438.
Butterfield, S.M., Lashuel, H.A., 2010. Amyloidogenic protein-membrane interactions: mechanistic insight from model systems. Angew. Chem. Int. Ed. Engl. 49, 5628–5654.
Diffenderfer, M.R., Schaefer, E.J., 2014. The composition and metabolism of large and small LDL. Curr. Opin. Lipidol. 25, 221–226.
Fang, Y., Gursky, O., Atkinson, D., 2003. Lipid-binding studies of human apolipoprotein A-I and its terminally truncated mutants. Biochemistry 42, 13260–13268.
Fisher, C.A., Ryan, R.O., 1999. Lipid binding-induced conformational changes in the N-terminal domain of human apolipoprotein E. J. Lipid Res. 40, 93–99.
Frame, N.M., Jayaraman, S., Gantz, D.L., Gursky, O., 2017. Serum amyloid A self-assembles with phospholipids to form stable protein-rich nanoparticles with a distinct structure: a hypothetical function of SAA as a "molecular mop" in immune response. J. Struct. Biol. 200, 293–302.
Gellermann, G.P., Appel, T.R., Tannert, A., Radestock, A., Hortschansky, P., Schroeckh, V., Leisner, C., Lutkepohl, T., Shtrasburg, S., Rocken, C., Pras, M., Linke, R.P., Diekmann, S., Fandrich, M., 2005. Raft lipids as common components of human extracellular amyloid fibrils. Proc. Natl. Acad. Sci. U. S. A. 102, 6297–6302.
Gomez Rosso, L., Lhomme, M., Merono, T., Sorroche, P., Catoggio, L., Soriano, E., Saucedo, C., Malah, V., Dauteuille, C., Boero, L., Lesnik, P., Robillard, P., John Chapman, M., Brites, F., Kontush, A., 2014. Altered lipidome and antioxidative activity of small, dense HDL in normolipidemic rheumatoid arthritis: relevance of inflammation. Atherosclerosis 237, 652–660.
Gursky, O., Ranjana, Gantz D.L., 2002. Complex of human apolipoprotein C-1 with phospholipid: thermodynamic or kinetic stability? Biochemistry 41, 7373–7384.
Hoffman, J.S., Benditt, E.P., 1982. Changes in high density lipoprotein content following endotoxin administration in the mouse. Formation of serum amyloid protein-rich subfractions. J. Biol. Chem. 257, 10510–10517.
Jayaraman, S., Gantz, D.L., Gursky, O., 2005. Kinetic stabilization and fusion of apolipoprotein A-2:DMPC disks: comparison with apoA-1 and apoC-1. Biophys. J. 88, 2907–2918.
Jayaraman, S., Haupt, C., Gursky, O., 2015. Thermal transitions in serum amyloid A in solution and on the lipid: implications for structure and stability of acute-phase HDL. J. Lipid Res. 56, 1531–1542.
Jayaraman, S., Gantz, D.L., Haupt, C., Fandrich, M., Gursky, O., 2018. Serum amyloid A sequesters diverse phospholipids and their hydrolytic products, hampering fibril formation and proteolysis in a lipid-dependent manner. Chem. Commun. (Camb.) 54, 3532–3535.
Jiang, Z., Hess, S.K., Heinrich, F., Lee, J.C., 2015. Molecular details of alpha-synuclein

membrane association revealed by neutrons and photons. J. Phys. Chem. B 119, 4812–4823.
Khovidhunkit, W., Kim, M.S., Memon, R.A., Shigenaga, J.K., Moser, A.H., Feingold, K.R., Grunfeld, C., 2004. Effects of infection and inflammation on lipid and lipoprotein metabolism: mechanisms and consequences to the host. J. Lipid Res. 45, 1169–1196.
Kolev, K., Dolashka-Angelova, P., 2001. Fluorescence studies on native and bound to trifluraline soy bean Lb"a" in the enhanced N2 fixation. Spectrochim. Acta A. Mol. Biomol. Spectrosc. 57, 2535–2545.
Lachmann, H.J., Goodman, H.J., Gilbertson, J.A., Gallimore, J.R., Sabin, C.A., Gillmore, J.D., Hawkins, P.N., 2007. Natural history and outcome in systemic AA amyloidosis. N. Engl. J. Med. 356, 2361–2371.
Lehrer, S.S., 1971. Solute perturbation of protein fluorescence. The quenching of the tryptophyl fluorescence of model compounds and of lysozyme by iodide ion. Biochemistry 10, 3254–3263.
Lu, J., Yu, Y., Zhu, I., Cheng, Y., Sun, P.D., 2014. Structural mechanism of serum amyloid A-mediated inflammatory amyloidosis. Proc. Natl. Acad. Sci. U. S. A 111, 5189–5194.
Lund-Katz, S., Phillips, M.C., 2010. High density lipoprotein structure-function and role in reverse cholesterol transport. Subcell. Biochem. 51, 183–227.
Marsche, G., Holzer, M., Wolf, P., 2014. Antipsoriatic treatment extends beyond the skin: recovering of high-density lipoprotein function. Exp. Dermatol. 23, 701–704.
Morgantini, C., Meriwether, D., Baldi, S., Venturi, E., Pinnola, S., Wagner, A.C., Fogelman, A.M., Ferrannini, E., Natali, A., Reddy, S.T., 2014. HDL lipid composition is profoundly altered in patients with type 2 diabetes and atherosclerotic vascular disease. Nutr. Metab. Cardiovasc. Dis. 24, 594–599.
Morita, S.Y., Ueda, K., Kitagawa, S., 2009. Enzymatic measurement of phosphatidic acid in cultured cells. J. Lipid Res. 50, 1945–1952.
Morita, S.Y., Takeuchi, A., Kitagawa, S., 2010. Functional analysis of two isoforms of phosphatidylethanolamine N-methyltransferase. Biochem. J. 432, 387–398.
Morita, S.Y., Shirakawa, S., Kobayashi, Y., Nakamura, K., Teraoka, R., Kitagawa, S., Terada, T., 2012a. Enzymatic measurement of phosphatidylserine in cultured cells. J. Lipid Res. 53, 325–330.
Morita, S.Y., Soda, K., Teraoka, R., Kitagawa, S., Terada, T., 2012b. Specific and sensitive enzymatic measurement of sphingomyelin in cultured cells. Chem. Phys. Lipids 165, 571–576.
Muller, D., Roessner, A., Rocken, C., 2000. Distribution pattern of matrix metalloproteinases 1, 2, 3, and 9, tissue inhibitors of matrix metalloproteinases 1 and 2, and alpha 2-macroglobulin in cases of generalized AA- and AL amyloidosis. Virchows Arch. 437, 521–527.
Narayanaswami, V., Ryan, R.O., 2000. Molecular basis of exchangeable apolipoprotein function. Biochim. Biophys. Acta 1483, 15–36.
Ohta, S., Tanaka, M., Sakakura, K., Kawakami, T., Aimoto, S., Saito, H., 2009. Defining lipid-binding regions of human serum amyloid A using its fragment peptides. Chem. Phys. Lipids 162, 62–68.
Ouyang, Y.S., Tu, Y., Barker, S.A., Yang, F., 2003. Regulators of G-protein signaling (RGS) 4, insertion into model membranes and inhibition of activity by phosphatidic acid. J. Biol. Chem. 278, 11115–11122.
Pollard, R.D., Fulp, B., Samuel, M.P., Sorci-Thomas, M.G., Thomas, M.J., 2013. The conformation of lipid-free human apolipoprotein A-I in solution. Biochemistry 52, 9470–9481.
Quezada, A.G., Diaz-Salazar, A.J., Cabrera, N., Perez-Montfort, R., Pineiro, A., Costas, M., 2017. Interplay between protein thermal flexibility and kinetic stability. Structure 25, 167–179.
Raja, M., Spelbrink, R.E., de Kruijff, B., Killian, J.A., 2007. Phosphatidic acid plays a special role in stabilizing and folding of the tetrameric potassium channel KcsA. FEBS Lett. 581, 5715–5722.
Rohamare, S.B., Gaikwad, S.M., 2014. Tryptophan environment and functional characterization of a kinetically stable serine protease containing a polyproline II fold. J. Fluoresc. 24, 1363–1370.
Ryan, T.M., Griffin, M.D., Teoh, C.L., Ooi, J., Howlett, G.J., 2011. High-affinity amphipathic modulators of amyloid fibril nucleation and elongation. J. Mol. Biol. 406, 416–429.
Saito, H., Dhanasekaran, P., Nguyen, D., Holvoet, P., Lund-Katz, S., Phillips, M.C., 2003. Domain structure and lipid interaction in human apolipoproteins A-I and E, a general model. J. Biol. Chem. 278, 23227–23232.
Segrest, J.P., Pownall, H.J., Jackson, R.L., Glenner, G.G., Pollock, P.S., 1976. Amyloid A: amphipathic helixes and lipid binding. Biochemistry 15, 3187–3191.
Shah, A.S., Tan, L., Long, J.L., Davidson, W.S., 2013. Proteomic diversity of high density lipoproteins: our emerging understanding of its importance in lipid transport and beyond. J. Lipid Res. 54, 2575–2585.
Stix, B., Kahne, T., Sletten, K., Raynes, J., Roessner, A., Rocken, C., 2001. Proteolysis of AA amyloid fibril proteins by matrix metalloproteinases-1, -2, and -3. Am. J. Pathol. 159, 561–570.
Takase, H., Furuchi, H., Tanaka, M., Yamada, T., Matoba, K., Iwasaki, K., Kawakami, T., Mukai, T., 2014. Characterization of reconstituted high-density lipoprotein particles formed by lipid interactions with human serum amyloid A. Biochim. Biophys. Acta 1842, 1467–1474.
Tanaka, M., Nishimura, A., Takeshita, H., Takase, H., Yamada, T., Mukai, T., 2017. Effect of lipid environment on amyloid fibril formation of human serum amyloid A. Chem. Phys. Lipids 202, 6–12.
Tolle, M., Huang, T., Schuchardt, M., Jankowski, V., Prufer, N., Jankowski, J., Tietge, U.J., Zidek, W., van der Giet, M., 2012. High-density lipoprotein loses its anti-inflammatory capacity by accumulation of pro-inflammatory-serum amyloid A. Cardiovasc. Res. 94, 154–162.
Uhlar, C.M., Whitehead, A.S., 1999. Serum amyloid A, the major vertebrate acute-phase reactant. Eur. J. Biochem. 265, 501–523.
van der Westhuyzen, D.R., de Beer, F.C., Webb, N.R., 2007. HDL cholesterol transport during inflammation. Curr. Opin. Lipidol. 18, 147–151.
Watanabe, J., Charles-Schoeman, C., Miao, Y., Elashoff, D., Lee, Y.Y., Katselis, G., Lee, T.D., Reddy, S.T., 2012. Proteomic profiling following immunoaffinity capture of high-density lipoprotein: association of acute-phase proteins and complement factors with proinflammatory high-density lipoprotein in rheumatoid arthritis. Arthritis Rheum. 64, 1828–1837.
Westermark, G.T., Westermark, P., 2009. Serum amyloid A and protein AA: molecular mechanisms of a transmissible amyloidosis. FEBS Lett. 583, 2685–2690.
Wilson, C., Wardell, M.R., Weisgraber, K.H., Mahley, R.W., Agard, D.A., 1991. Three-dimensional structure of the LDL receptor-binding domain of human apolipoprotein E. Science 252, 1817–1822.
Yamada, T., Wada, A., 2003. Slower clearance of human SAA1.5 in mice: implications for allele specific variation of SAA concentration in human. Amyloid 10, 147–150.